Frontiers of Optoelectronics (2022) 15:5
https://doi.org/10.1007/s12200-022-00008-5

Frontiers *of* Optoelectronics

RESEARCH ARTICLE

Check for updates

# An ultra-compact polarization-insensitive slot-strip mode converter

Zihan Tao[1] · Bo Wang[1] · Bowen Bai[1] · Ruixuan Chen[1] · Haowen Shu[1] · Xuguang Zhang[1] · Xingjun Wang[1,2,3,4]

Received: 30 August 2021 / Accepted: 2 November 2021 / Published online: 2 April 2022


**Abstract**

Integrated waveguides with slot structures have attracted increasing attention due to their advantages of tight mode confinement and strong light-matter interaction. Although extensively studied, the issue of mode mismatch with other strip waveguide-based optical devices is a huge challenge that prevents integrated waveguides from being widely utilized in large-scale photonic-based circuits. In this paper, we demonstrate an ultra-compact low-loss slot-strip converter with polarization insensitivity based on the multimode interference (MMI) effect. Sleek sinusoidal profiles are adopted to allow for smooth connection between the slot and strip waveguide, resulting reflection reduction. By manipulating the MMI effect with structure optimization, the self-imaging positions of the $TE_0$ and $TM_0$ modes are aligned with minimized footprint, leading to low-loss transmission for both polarizations. The measurement results show that high coupling efficiencies of − 0.40 and − 0.64 dB are achieved for $TE_0$ and $TM_0$ polarizations, respectively. The device has dimensions as small as 1.1 μm × 1.2 μm and composed of factory-available structures. The above characteristics of our proposed compact slot-strip converter makes it a promising device for future deployment in multi-functional integrated photonics systems.

**Keywords** Silicon photonics · Slot-strip convertor · Multimode interference (MMI) · Polarization-insensitive

## 1 Introduction

Silicon photonics is emerging as an extensively universal platform due to their integration of various low cost, high-density photonic devices and the maturity of complementary metal-oxide semiconductor (CMOS) manufacturing technology [1–4]. Silicon-based slot waveguides are constructed with a narrow low-index slot ($SiO_2$ or air) embedded between two high-index silicon waveguides. Owing to their unique optical field distributions [5–7], slot waveguides are irreplaceable in many applications, such as optical sensors [6], high speed modulators [8, 9], polarization controlling devices [10–12], and nonlinear optical devices [13]. However, the propagation loss of slot waveguides, which is almost one order of magnitude larger than that of strip waveguides [14, 15], poses serious challenges for realizing low loss photonic circuits based solely on slot waveguides. Thus, a compact slot-strip converter is necessary to effectively connect the slot waveguide-based functional device with other photonic components. To date, various schemes have been proposed to achieve high coupling efficiency for slot-strip converters. The adiabatic evolution structure [16–18] is widely used while the sharp tips cannot be avoided during gradual mode conversion, which pose great challenges for high-precision fabrication. For example, multimode interference (MMI) schemes [19, 20] produce reflections due to mutation of the waveguide. Moreover, overly narrow slots (which also existed in Ref. [21]) and non-standard silicon thicknesses also make large-scale production extremely difficult, not to mention the advanced fabrication process. Furthermore, the compactness of most schemes is insufficient. Despite its numerous challenges, polarization multiplexing technology is still an effective approach to enhance the capacity of on-chip optical interconnects [22], making polarization-insensitive mode converters [20] paramount for applications that involve multiple modes [12, 23].

✉ Xingjun Wang
xjwang@pku.edu.cn

1 State Key Laboratory of Advanced Optical Communication Systems and Networks, School of Electronics, Peking University, Beijing 100871, China

2 Frontier Science Center for Nano-Optoelectronics, Peking University, Beijing 100871, China

3 Peking University Yangtze Delta Institute of Optoelectronics, Nantong 226010, China

4 Peng Cheng Laboratory, Shenzhen 518055, China

In this paper, a polarization-insensitive slot-strip converter is proposed and demonstrated based on novel sinusoidal-profile MMI, which not only decreases the optical mode field mismatching but also has an ultra-compact device size. The insertion losses for $TE_0$ and $TM_0$ polarizations are measured as low as 0.40 and 0.64 dB, respectively. The polarization-dependent loss is 0.24 dB, indicating that the converter can handle a variety of applications where both $TE_0$ and $TM_0$ polarizations are needed. Theories and preliminary simulation results have been roughly investigated in Ref. [24], while this paper will present more detailed principles, simulation, and experimental results.

## 2 Design and principles

As illustrated in Figs. 1(a) and (b), the proposed converter is based on a silicon-on-insulator (SOI) platform, with a 220 nm top Si and 2 μm $SiO_2$ cladding. The width ($W_i$) of the slot waveguide is set at 300 nm for specific needs and the gap ($g$) is fixed at 200 nm, which is compatible with standard 180 nm CMOS processes. The output strip waveguide width ($W_o$) is 400 nm for single mode operation. The core region, where the MMI effect and optical mode evolution take place from slot mode to strip mode, is shown in Fig. 1(d). In the calculation, $\{E_{tv}, H_{tv}\}$ represent the transverse optical fields of the slot waveguide, while that of the eigenmodes in the MMI region is denoted as $\{E_{tm}, H_{tm}\}$. Based on the coupled mode theory, the mode overlap ratio (Γ) between the two structures can be described as

$$\Gamma = \frac{\left|\frac{1}{4}\iint [E_{tm} \times H_{tv}^* + E_{tv}^* \times H_{tm}]_z \mathrm{d}x\mathrm{d}y\right|^2}{\frac{1}{4}\iint [E_{tv} \times H_{tv}^* + E_{tv}^* \times H_{tv}]_z \mathrm{d}x\mathrm{d}y \cdot \frac{1}{4}\iint [E_{tm} \times H_{tm}^* + E_{tm}^* \times H_{tm}]_z \mathrm{d}x\mathrm{d}y}. \quad (1)$$

According to Eq. (1), the $TE_0$ of slot mode can be expanded into $TE_0$ and $TE_2$ of strip mode in the MMI region and the self-imaging points would be periodically

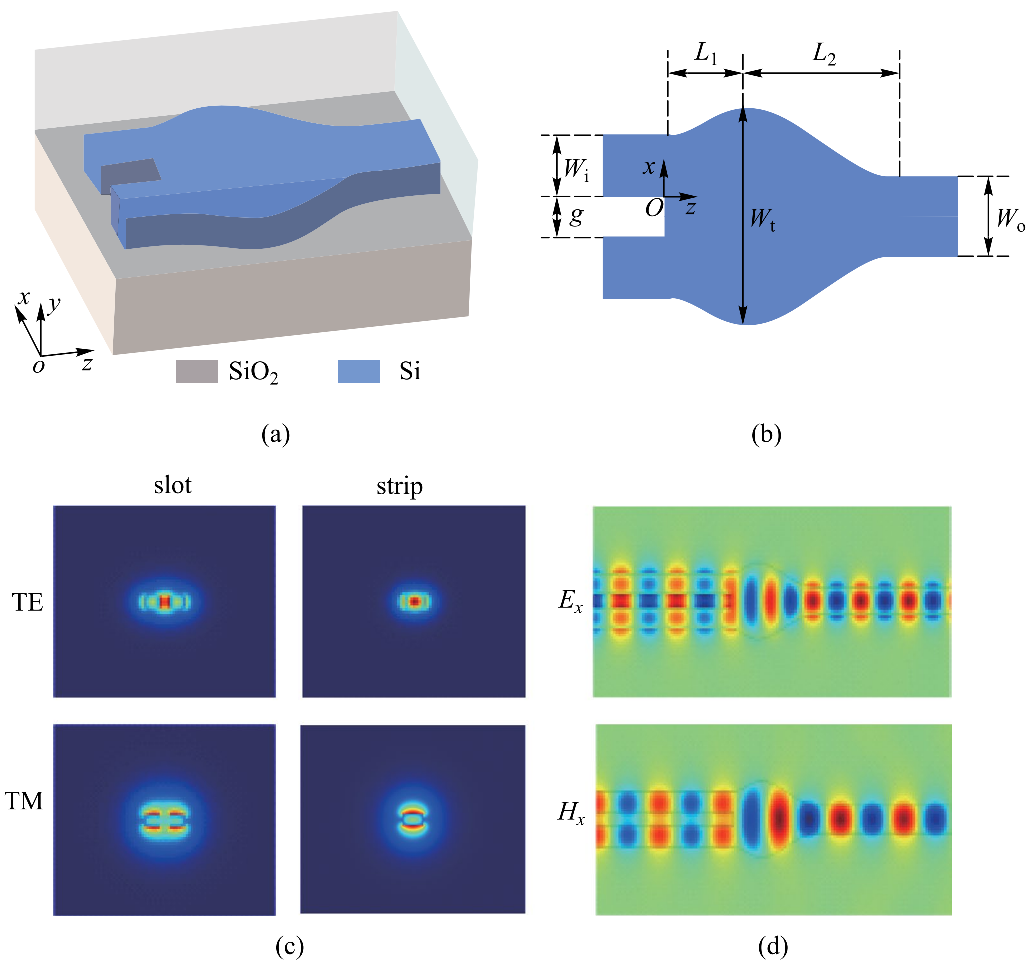


**Fig. 1** **a** 3D schematic of the device. **b** 2D schematic of the device with structural parameters. **c** 2D optical mode distribution on cross section of slot and strip waveguides. **d** Optical field ($E_x$ or $H_x$) evolution with the input of slot waveguide and output of strip waveguide for both $TE_0$ and $TM_0$ respectively

restructured. For the 800 nm width strip waveguide, the proportion of $TE_0$ and $TE_2$ is 89.7% and 7.6%, respectively, when the slot mode is injected. The MMI process differs from the previous MMI principle in that the proposed structure is spatially modulated by the profile. Thus, the propagation constant of each mode is variable and the position and proportion of different onefold image modes are different with each change of profile. Therefore, by appropriately designing the shape of the sinusoidal-MMI region, the desired mode distribution can be obtained at the output port.

The core region is composed of two different sinusoids with longitudinal lengths of $L_1$ and $L_2$. The junction of these two arcs determines the maximum width ($W_t$). The function of the profile is

$$x = \frac{W_t - 2W_i - g}{4} \sin\left(\frac{\pi}{L_1}z - \frac{\pi}{2}\right) + C_0,\ z \in (0, L_1],$$

and

$$x = \frac{W_t - W_o}{4} \sin\left(\frac{\pi}{L_2}z + \frac{\pi}{2}\right) + C_1,\ z \in (L_1, L_2].$$

The first order derivative of the sinusoidal arcs is zero at points $-\pi/2$ and $\pi/2$, which forms a smooth mode transition at the butt-joint area between the slot waveguide and MMI region for reflection reduction. To demonstrate this theory, a conventional structure in which a slot waveguide directly couples to a regular rectangle waveguide (1.2 μm width) as the MMI region was simulated. In comparison, the proposed structure can theoretically achieve a 30% reflection reduction. Other core region profiles in reality demonstrate geometric similarities when the first order derivative is zero. The differences between these structures may not be as apparent following production. Since high performance have been obtained with a sinusoidal function, this simple and easily available profile function was adopted. While previous structures require a tapered structure after the MMI/directly coupling region for single mode operation, our proposed structure does not require the additional tapered region to function, allowing for further size reduction. This is because our design combines the functions of both regions, so that the optical field can be manipulated inside the sinusoidal-MMI and the mode profile of the MMI onefold image highly overlaps with that in the 400 nm single-mode waveguide.

The ideal way to achieve polarization-insensitive mode conversion is to calculate the self-imaging positions of $TE_0$ and $TM_0$, where polarization constructs the onefold images. However, this may result in a larger device size since the coincident point may be located further from the starting position. In our design, the first onefold image for both $TE_0$ and $TM_0$ is the optimal solution because the relatively small distance between the two points can still guarantee low-loss transmission of both polarizations. Optimization of the core region structure was achieved through parameter traversing of $\{W_t, L_1, L_2\}$ around the first onefold image as shown in Figs. 2(a) and (b), where the figure of merit (FOM) is defined as

$$\mathrm{FOM} = T_{\mathrm{TE}} \times T_{\mathrm{TM}}, \quad (2)$$

where $T_{\mathrm{TE}}$ ($T_{\mathrm{TM}}$) represent the normalized transmission of $TE_0$ ($TM_0$). A high FOM indicates high transmission for both $TE_0$ and $TM_0$ polarizations. Finally, dimensions of $W_t = 1.1$ μm, $L_1 = 0.4$ μm, and $L_2 = 0.8$ μm were selected for low-loss polarization-insensitive slot-strip conversion. All 3D simulations presented in this paper were carried out using finite element method (FEM). Figure 2(c) and (d) show the fabrication tolerance analysis. The waveguide width variation, $\Delta W$ (including the variation of $W_i$, $W_t$, and $W_o$), and the slot gap variation, $\Delta g$, are significant parameters when determining the fabrication tolerance. The simulation results indicate that the conversion efficiency decline are less than 0.3% for $TE_0$ mode, 0.7% for $TM_0$ mode with the variation of $g$ within ± 20 nm, and 2.1% for $TE_0$, 1.4% for $TM_0$ with the variation of $W$ within ± 20 nm.

## 3 Fabrication and experimental measurements

The proposed converter was fabricated in the United Microelectronics Center (CUMEC), based on standard 180 nm SiP process (Fig. 3(a)). Figure 3(b) exhibits the scanning electron microscope (SEM) image of the converter. The total length of the proposed converter is 1.2 μm. A polarization-sensitive grating coupler was used to guide the light into the chip, while maintaining high polarization selectivity for either $TE_0$ or $TM_0$ modes. To characterize device performance, a tunable continuous wave (CW) laser (AQ 2200-136TLS, YOKOGAWA) was used as the source and the polarization was adjusted using a polarization controller (DPC5500, THORLABS). Then, the light was coupled into the chip through the polarization-sensitive grating coupler. An optical spectrum analyzer (AQ 6370C, YOKOGAWA) was used to measure the output spectrum coupled from the output grating coupler. Figure 3(c) shows the measured transmission for both $TE_0$ and $TM_0$ modes, which are extracted by normalizing the measured spectra with a 400 nm width waveguide to exclude the loss of grating coupling.

The normalized spectra still show a small amount of reflection from the butt-joint since the ripple of the spectrum especially for $TE_0$, is observed as a result of Fabry–Perot resonance. The robust locally weighted regression method has been implemented [25] to suppress the noise (shown as solid black lines in Fig. 3(c)). The insertion loss (IL), defined as

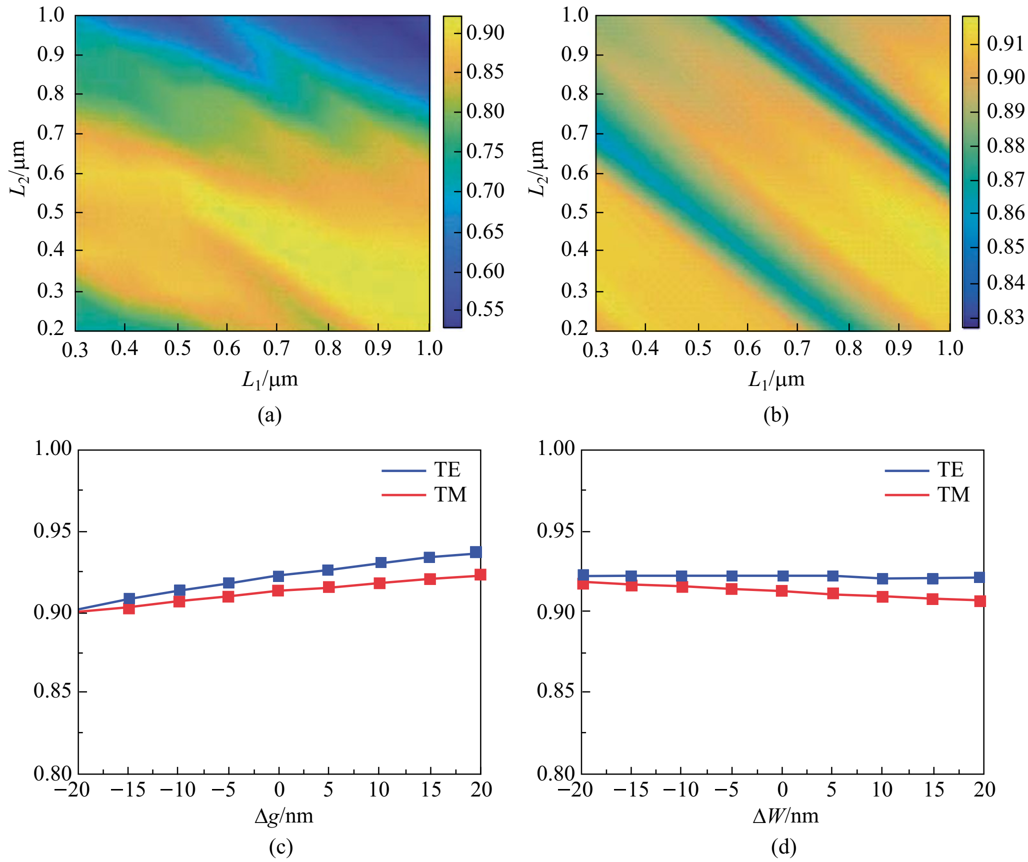


**Fig. 2** Simulation results of **a** $TE_0$ and **b** $TM_0$ normalized transmission with different lengths of $L_1$ and $L_2$ under the width $W_t$ of 1.1 μm. **c** and **d** show the simulation results of fabrication tolerance

$IL_{TE_0,TM_0} = 10\log_{10}\left(P_{TE_0,TM_0}/P_{in}\right)$, is used to characterize the transmission loss. At approximately the 1550 nm wavelength, the IL is – 0.40 and – 0.64 dB (single-ended loss) for $TE_0$ and $TM_0$, respectively, indicating that the proposed converter is capable of low loss transmission for both polarizations. The polarization-dependent loss (PDL), defined as $PDL = |IL_{TE} - IL_{TM}|$, is used to characterize the polarization insensitivity of the converter. The PDL of the converter is about 0.24 dB, meaning it can support most polarization-insensitive applications. Compared to other studies, the converter proposed in this paper is the most compact in size, though the IL may be slightly lower than others in Refs. [19, 20]. However, according to the coupled mode theory, a wider slot can exacerbate mode mismatch, as illustrated in Ref. [21]. With that said, we still need to overcome many challenges in order to eliminate mode mismatch for a 200 nm slot, the widest of all previous works.

## 4 Conclusion

In conclusion, this paper numerically and experimentally demonstrates an ultra-compact polarization-insensitive slot-strip converter that takes advantage of low-loss transmission of the MMI effect. Due to the characteristic shape of the sinusoidal arcs, the converter can create a smooth connection between the slot and single-mode strip waveguide, with only slight reflections. The proposed device is easily manufactured, with a compact dimensions of 1.1 μm × 1.2 μm. The IL for both $TE_0$ and $TM_0$ polarizations is lower than 0.65 dB and the PDL is about 0.24 dB at around 1550 nm. These characteristics are advantageous for various applications that require both $TE_0$ and $TM_0$ polarizations, such as optical sensing, high speed modulation, and polarization controlling devices.

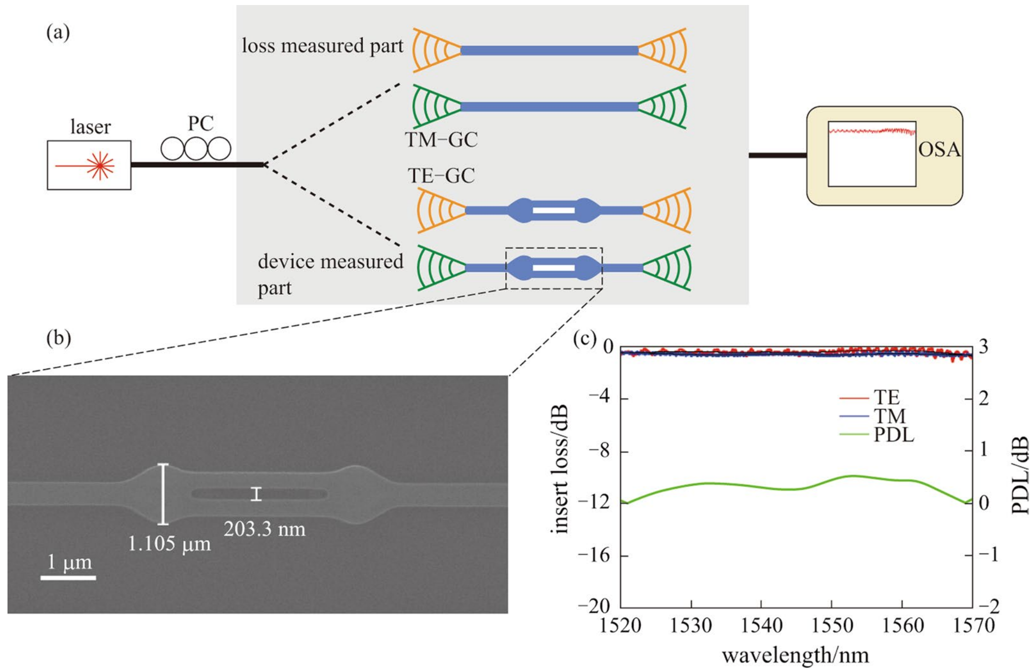


**Fig. 3** **a** Schematic of the device measurement. PC, polarization control; TM-GC, TM polarization sensitive grating coupler; TE-GC, TE polarization sensitive grating coupler; OSA, optical spectrum analyzer. **b** Top-view SEM picture of fabricated converters. **c** Measured transmission of $TE_0$ mode (red line) and $TM_0$ mode (blue line); the black line are trend lines by robust locally weight regression method. The green line represents the polarization dependent loss (PDL)

**Acknowledgements** This work was funded by the National Key Research and Development Program of China (No. 2018YFB2201704), the National Natural Science Foundation of China (Grant Nos. 61635001 and 62105008), China National Postdoctoral Program for Innovative Talents (No. BX20200017), China Postdoctoral Science Foundation (No. 2021T140004), the Major Key Project of PCL (No. PCL2021A14). We would like to thank Yuansheng Tao, Ming Jing, and Bitao Shen for their fruitful discussions, and Ziyi Wei for taking the SEM images.

**Authors' contributions** The authors read and approved the final manuscript.

## Declarations

**Competing interests** The authors declare that they have no competing interests.



## References

1. Soref, R.: The past, present, and future of silicon photonics. IEEE J. Sel. Top. Quantum Electron. **12**(6), 1678–1687 (2006)
2. Jalali, B., Fathpour, S.: Silicon photonics. J. Lightwave Technol. **24**(12), 4600–4615 (2006)
3. Bai, B., Shu, H., Wang, X., Zou, W.: Towards silicon photonic neural networks for artificial intelligence. Sci. China Inf. Sci. **63**(6), 160403 (2020)
4. Shen, B., Shu, H., Zhou, L., Wang, X.: A design method for high fabrication tolerance integrated optical mode multiplexer. Sci. China Inf. Sci. **63**(6), 160409 (2020)
5. Almeida, V.R., Xu, Q., Barrios, C.A., Lipson, M.: Guiding and confining light in void nanostructure. Opt. Lett. **29**(11), 1209–1211 (2004)
6. Dell'Olio, F., Passaro, V.M.N.: Optical sensing by optimized silicon slot waveguides. Opt. Express **15**(8), 4977–4993 (2007)

7. Yamada, H., Chu, T., Ishida, S., Arakawa, Y.: Si photonic wire waveguide devices. IEEE J. Sel. Top. Quantum Electron. **12**(6), 1371–1379 (2006)
8. Ding, R., Baehr-Jones, T., Liu, Y., Bojko, R., Witzens, J., Huang, S., Luo, J., Benight, S., Sullivan, P., Fedeli, J.M., Fournier, M., Dalton, L., Jen, A., Hochberg, M.: Demonstration of a low $V_{\pi}L$ modulator with GHz bandwidth based on electro-optic polymer-clad silicon slot waveguides. Opt. Express **18**(15), 15618–15623 (2010)
9. Phatak, A., Cheng, Z., Qin, C., Goda, K.: Design of electro-optic modulators based on graphene-on-silicon slot waveguides. Opt. Lett. **41**(11), 2501–2504 (2016)
10. Zheng, Z., Iqbal, M., Liu, J.: Dispersion characteristics of SOI-based slot optical waveguides. Optics Commun. **281**(20), 5151–5155 (2008)
11. Shu, H., Deng, Q., Jin, M., Tao, Y., Wang, X., Zhou, Z. Efficient graphene phase modulator based on a polarization multiplexing optical circuit. In: Proceedings of Optical Fiber Communication Conference. Optical Society of America, W2A.9 (2019)
12. Deng. Q., Liu, L., Zhou, Z. Experimental demonstration of an ultra-compact on-chip polarization controlling structure. arXiv preprint arXiv:1705.10275 (2017)
13. Shu, H., Deng, Q., Wang, X., Jin, M., Tao, Y., Zhou, Z.: A polarization multiplexing optical circuit for efficient phase tuning. IEEE Photonics Technol. Lett. **31**(19), 1549–1552 (2019)
14. Hochberg, M., Baehr-Jones, T., Wang, G., Huang, J., Sullivan, P., Dalton, L., Scherer, A.: Towards a millivolt optical modulator with nano-slot waveguides. Opt. Express **15**(13), 8401–8410 (2007)
15. Thylén, L., Wosinski, L.: Integrated photonics in the 21st century. Photonics Res. **2**(2), 75–81 (2014)
16. Zhang, H., Zhang, J., Chen, S., Song, J., Kee, J.S., Yu, M., Lo, G.Q.: CMOS-compatible fabrication of silicon-based sub-100-nm slot waveguide with efficient channel-slot coupler. IEEE Photonics Technol. Lett. **24**(1), 10–12 (2012)
17. Wang, Z., Zhu, N., Tang, Y., Wosinski, L., Dai, D., He, S.: Ultracompact low-loss coupler between strip and slot waveguides. Opt. Lett. **34**(10), 1498–1500 (2009)
18. Feng, N.N., Sun, R., Kimerling, L.C., Michel, J.: Lossless strip-to-slot waveguide transformer. Opt. Lett. **32**(10), 1250–1252 (2007)
19. Deng, Q., Liu, L., Li, X., Zhou, Z.: Strip-slot waveguide mode converter based on symmetric multimode interference. Opt. Lett. **39**(19), 5665–5668 (2014)
20. Deng, Q., Yan, Q., Liu, L., Li, X., Michel, J., Zhou, Z.: Robust polarization-insensitive strip-slot waveguide mode converter based on symmetric multimode interference. Opt. Express **24**(7), 7347–7355 (2016)
21. Han, K., Kim, S., Wirth, J., Teng, M., Xuan, Y., Niu, B., Qi, M.: Strip-slot direct mode coupler. Opt. Express **24**(6), 6532–6541 (2016)
22. Zhou, Z., Bai, B., Liu, L.: Silicon on-chip PDM and WDM technologies via plasmonics and subwavelength grating. IEEE J. Sel. Top. Quantum Electron. **25**(3), 1–13 (2018)
23. Chen, R., Bai, B., Zhou, Z.: Low-loss hybrid plasmonic TM-pass polarizer using polarization-dependent mode conversion. Photonics Res. **8**(7), 1197–1202 (2020)
24. Tao, Z., Bai, B., Chen, R., Wang, X.: Adiabatic slot-to-strip waveguide mode converters based on self-imaging effect of MMI structures. In: Proceedings of Asia Communications and Photonics Conference. Optical Society of America, M4A.146 (2020)
25. Cleveland, W.S.: Robust locally weighted regression and smoothing scatterplots. J. Am. Stat. Assoc. **74**(368), 829–836 (1979)

**Zihan Tao** Received his bachelor's degree from Xidian University, China in 2020, and is currently studying for a PhD in Peking University, China. His research interest is silicon-based integrated microwave photonics.

**Bo Wang** Received his bachelor's degree from Peking University, China in 2018, and is currently studying for a PhD in Peking University, China. His research interest is silicon based laser.

**Bowen Bai** Received his bachelor's degree from University of Electronic Science and Technology of China, China in 2014, and PhD degree from Peking University, China in 2019. Currently, he is working in State Key Laboratory of Advanced Optical Communication System and Networks, Peking University. His research interest is on-chip photonic neural network.

**Ruixuan Chen** Received his bachelor's degree from University of Electronic Science and Technology of China, China in 2015, and PhD degree from Peking University, China in 2020. Currently, as a postdoctor he is working in State Key Laboratory of Advanced Optical Communication System and Networks, Peking University. His research interest is silicon based polarization control device, on-chip Lidar.

**Haowen Shu** Received his bachelor's degree from Beijing University of Posts and Telecommunications, China in 2015, and PhD degree from Peking University, China in 2020. Currently, as a postdoctor he is working in State Key Laboratory of Advanced Optical Communication System and Networks, Peking University. His research interest is microcavity optical frequency comb and applications.

**Xuguang Zhang** Received his bachelor's degree from Zhengzhou University, China in 2018, and is currently studying for a PhD in Peking University, China. His research interest is silicon based laser.

**Xingjun Wang** Is professor, doctoral supervisor at Peking University, China, deputy director of Department of Electronics and State Key Laboratory of Regional Optical Fiber Communication Networks and New Optical Communication Systems, Ministry of Education New Century Excellent Talents (2013), National Natural Science Foundation of China Key Project Leader, Ministry of Science and Technology 863 Major Project Leader, Science and Technology Commission High-Tech Key R&D Project Leader. His research interest is photonic chip and information system.